AIP Journal of Applied Physics

Effect of uniaxial stress on ferroelectric behavior of (Bi 1 / 2 Na 1 / 2) TiO 3 -based lead-free piezoelectric ceramics

X. Tan, E. Aulbach, W. Jo, T. Granzow, J. Kling, M. Marsilius, H.-J. Kleebe, and J. Rödel

Citation: Journal of Applied Physics **106**, 044107 (2009); doi: 10.1063/1.3207827
View online: http://dx.doi.org/10.1063/1.3207827
View Table of Contents: http://scitation.aip.org/content/aip/journal/jap/106/4?ver=pdfcov
Published by the AIP Publishing

Effect of uniaxial stress on ferroelectric behavior of $(Bi_{1/2}Na_{1/2})TiO_3$-based lead-free piezoelectric ceramics

X. Tan,[1,a] E. Aulbach,[2] W. Jo,[2] T. Granzow,[2] J. Kling,[2] M. Marsilius,[2] H.-J. Kleebe,[2] and J. Rödel[2]
[1]*Department of Materials Science and Engineering, Iowa State University, Ames, Iowa 50011, USA*
[2]*Institute of Materials Science, Technische Universität Darmstadt, 64287 Darmstadt, Germany*

(Received 10 April 2009; accepted 22 July 2009; published online 31 August 2009)

Prior studies have shown that a field-induced ferroelectricity in ceramics with general chemical formula $(1-x-y)(Bi_{1/2}Na_{1/2})TiO_3-xBaTiO_3-y(K_{0.5}Na_{0.5})NbO_3$ and a very low remanent strain can produce very large piezoelectric strains. Here we show that both the longitudinal and transverse strains gradually change with applied electric fields even during the transition from the nonferroelectric to the ferroelectric state, in contrast to known Pb-containing antiferroelectrics. Hence, the volume change and, in turn, the phase transition can be affected using uniaxial compressive stresses, and the effect on ferroelectricity can thus be assessed. It is found that the $0.94(Bi_{1/2}Na_{1/2})TiO_3-0.05BaTiO_3-0.01(K_{0.5}Na_{0.5})NbO_3$ ceramic (largely ferroelectric), with a rhombohedral *R*3*c* symmetry, displays large ferroelectric domains, significant ferroelastic deformation, and large remanent electrical polarizations even at a 250 MPa compressive stress. In comparison, the $0.91(Bi_{1/2}Na_{1/2})TiO_3-0.07BaTiO_3-0.02(K_{0.5}Na_{0.5})NbO_3$ ceramic (largely nonferroelectric) possesses characteristics of a relaxor ferroelectric ceramic, including a pseudocubic structure, limited ferroelastic deformation, and low remanent polarization. The results are discussed with respect of the proposed antiferroelectric nature of the nonferroelectric state.
 [DOI: 10.1063/1.3207827]

I. INTRODUCTION

For the past 5 decades, Pb-containing perovskite oxides have been the workhorse of piezoelectric technology due to their excellent properties, ease of processing, and low cost.[1] However, environmental concerns with lead have stimulated intensive search for lead-free piezoelectric ceramics worldwide.[2] These research efforts have been largely focused on ceramics based on $(K_{0.5}Na_{0.5})NbO_3$ (KNN) and $(Bi_{1/2}Na_{1/2})TiO_3$ (BNT), and piezoelectric coefficient d_{33} values close to that of Pb-containing ceramics have been reported.[3–11] While d_{33} is an important benchmark value in piezoelectric ceramics, it is not the decisive quantity in all applications: for actuator applications, it is often desirable to have large field-induced strain, even when the remanent polarization and correspondingly d_{33} at zero field is small. We recently observed giant electric field-induced strains (up to 0.45%) in ceramics of the $(1-x-y)(Bi_{1/2}Na_{1/2})TiO_3-xBaTiO_3-y(K_{0.5}Na_{0.5})NbO_3$ system.[12–14] Near the morphotropic phase boundary at around 6 mol % $BaTiO_3$ (BT), $(Bi_{1/2}Na_{1/2})TiO_3-BaTiO_3$ exhibits field-induced ferroelectricity and remains ferroelectric after field removal.[15] The related ceramics containing small amounts of KNN display giant strains due to the full recovery of the original dimensions for every electric cycle.[16] However, the nature of the field-free state is still questionable. Literature traditionally suggests that BNT-BT has an antiferroelectric high-temperature phase.[4] Presumably, the addition of KNN lowers the depolarization temperature, i.e., the transition temperature from the low-temperature ferroelectric to the high-temperature antiferroelectric phase. The large electric field-induced strain in BNT-BT-KNN was attributed to a field-induced transition from the antiferroelectric to the ferroelectric phase that was supposed to be connected to a change in the unit cell volume. This is in close analogy to observations on lead-containing antiferroelectric ceramics. However, recent observations have cast some doubts on the designation of the field-free nonferroelectric high-temperature phase as "antiferroelectric." While the low-temperature phase and the field-induced phase are probably indeed ferroelectric,[15] and there is a transition to a high-temperature phase,[14] the volume change during the proposed transition was observed but could account only for a small amount of the observed total strain.[16] Furthermore, some of the typical features of antiferroelectrics such as antiferroelectric domains could not be evidenced so far. The question therefore remains unsolved to what degree the field-induced ferroelectricity itself contributes to field-induced strain.

When used in practical devices, such as transducers or actuators, these lead-free piezoelectric ceramics will be subjected to combined mechanical and electrical loads. Furthermore, high blocking stresses are always desired for piezoelectric actuators.[2] Therefore, knowledge of how added mechanical constraints influence the electrical properties of these lead-free ceramics becomes essential. It is highly likely that the driving force for the volume change specifically can be influenced by uniaxial compressive prestresses.

The effects of mechanical stresses on electromechanical properties in Pb-containing piezoelectric ceramics have been extensively studied.[17–22] However, similar studies on lead-

[a]Author to whom correspondence should be addressed. Electronic mail: xtan@iastate.edu.

free piezoelectric ceramics have not yet been reported. Since these lead-free piezoelectric ceramics with the perovskite structure display non-180° ferroelectric domains as well,[23] the ferroelastic nature of these domains and the intrinsic piezoelectric lattice response render them responsive to mechanical stresses. The present work focuses on the effect of uniaxial compressive stresses on the ferroelectric behavior at different temperatures in the $(1-x-y)(Bi_{1/2}Na_{1/2})TiO_3-xBaTiO_3-y(K_{0.5}Na_{0.5})NbO_3$ lead-free system. To highlight the salient physics and to investigate the nature of the nonferroelectric phase, two compositions were chosen: one was predominantly ferroelectric at room temperature. The other one belonged to the nonferroelectric phase that has been referred to as antiferroelectric so far.[13,14]

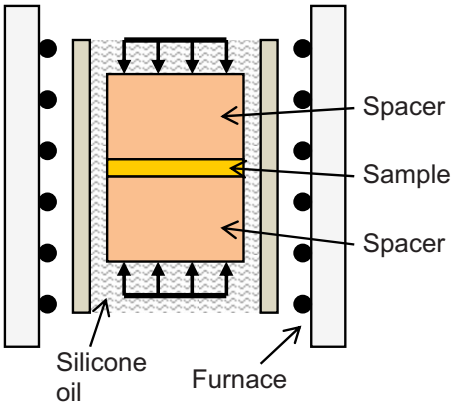

FIG. 1. (Color online) Schematic diagram of the experimental setup for the measurement of polarization hysteresis loops under uniaxial compressive prestresses.

II. EXPERIMENTAL PROCEDURE

Ceramics with compositions of $0.94(Bi_{1/2}Na_{1/2})TiO_3-0.05BaTiO_3-0.01(K_{0.5}Na_{0.5})NbO_3$ (abbreviated as BNT-FE for the dominating ferroelectric feature) and $0.91(Bi_{1/2}Na_{1/2})TiO_3-0.07BaTiO_3-0.02(K_{0.5}Na_{0.5})NbO_3$ were selected for the present study. The latter composition will be referred to as BNT-AFE: it has antiferroelectric features; note that the nature of the AFE phase is still open. Our previous work indicated that BNT-FE displays a higher T_d and is ferroelectric at room temperature, while BNT-AFE appears largely antiferroelectric at room temperature.[13,14] The two ceramics were prepared with the conventional solid state reaction method. Sintering was carried out at 1150 °C for 3 h with pellets buried in the powder of the same composition in covered alumina crucibles.

Transmission electron microscopy (TEM) was utilized to verify the different microstructures of both ceramics. Specimen preparation followed standard procedures which include cutting, grinding, polishing, and ion milling. Perforated thin foils were coated with carbon to minimize charging under electron beam illumination during observation. Conventional bright field imaging and selected area electron diffraction were performed on a Philips CM12 instrument (FEI Eindhoven, The Netherlands) operating at 120 kV.

Disk shaped samples with a diameter of 7.0 mm and a thickness of 1.0 mm were prepared to measure piezoelectric strains. After polishing and lapping, the circular faces of the disk samples were electroded with Ag films by sputtering. The electric field was applied along the thickness direction, using a triangular waveform with a frequency of 50 mHz. Three linear variable displacement transducers were used to measure the electric field-induced strains: one for the longitudinal strain x_{33} in the thickness direction, and two for the transverse strain x_{11} in the radial direction. During the measurement, the signals (electric field E, longitudinal strain x_{33}, and transverse strain x_{11}) were collected and recorded simultaneously with a multichannel oscilloscope.

Identical samples were also used for the measurement of the field-induced polarization and the determination of the depolarization temperature. For the depolarization measurement, the samples were heated to 150 °C in a silicone oil bath and then a static field of 45 kV/cm was applied. The samples were poled when they cooled down to room temperature with the static field on. The field was removed, and the samples were connected to an electrometer (model 6514, Keithley Corporate, Cleveland, OH). The thermal depolarization current was monitored as they were warmed up to 150 °C at a rate of 0.6 °C/min.

Large ceramic cylindrical samples 7.5 mm in diameter and 16.0 mm in height were prepared for the determination of ferroelasticity. The two end faces of the samples were lapped to ensure parallelism. The test was conducted on a hydraulic testing machine (MTS 810.22, Materials Test Systems Corporation, Minneapolis, MN) with the load-control mode at a loading/unloading rate of 50 N/s. A special test fixture with a top spherical joint was used to ensure good alignment. The mechanical strain along the loading axial direction was monitored and recorded with an extensometer (model 3442/006 m, Epsilon Technology Corporation, Jackson, WY).

Disk samples (diameter of 7.0 mm and thickness of 1.0 mm) were also lapped to obtain parallel and flat faces for the measurement of polarization versus electric field hysteresis loops under uniaxial compressive prestresses. In order to minimize the end clamp effect and ensure a uniform uniaxial stress state in the testing sample,[24,25] the disk sample was sandwiched between two thicker ceramic disks of the same composition (diameter of 7.0 mm and thickness of 4.0 mm). The triblock assembly was loaded to a special fixture made of Teflon for good alignment and electrical insulation, as schematically shown in Fig. 1. Upon heating, the BNT-FE sample is expected to transform into the nonferroelectric phase region at temperature T_d, which afforded investigation of the effect of electromechanical loading on properties not only for different compositions but also for different temperatures. Hence, the polarization hysteresis loops were measured under a series of uniaxial compressive prestresses at 25, 80 and 140 °C for both ceramics. Electrical measurements were taken 30 min after the temperature was stabilized in order to achieve uniform temperature in the test sample. The mechanical load was applied at a rate of 50 N/s to a predetermined stress value in the load control mode. During heating and mechanical loading, the two electrodes of the sample were shortened. The applied electric field for the hysteresis loop measurement took a triangular form with a fre-

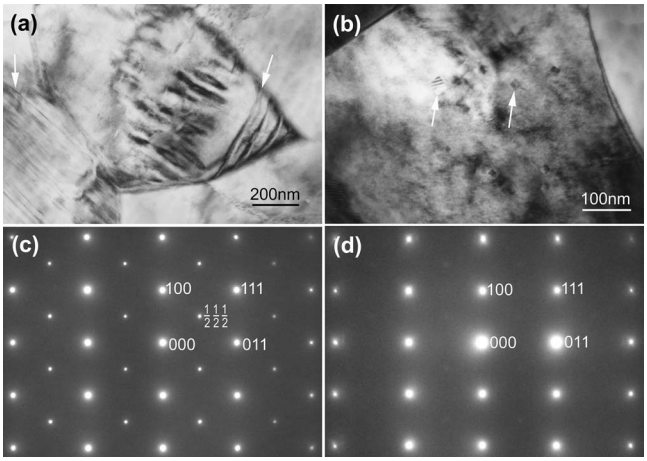

FIG. 2. The domain morphology and crystal structure in BNT-FE and BNT-AFE at room temperature revealed by TEM. (a) The large ferroelectric/ferroelastic domains and (c) the $(\frac{1}{2}\frac{1}{2}\frac{1}{2})$ superlattice diffractions spots in BNT-FE. (b) The nanometer sized defects and (d) the extremely weak superlattice spots in BNT-AFE.

quency of 50 mHz. The low frequency was used to ensure that the electric field-induced strain can be accommodated by the mechanical loading frame and a constant stress is maintained during the hysteresis loop measurement.

III. RESULTS

A. Domain morphology and crystal structure

Figure 2 shows the TEM observations of both compositions at room temperature. In our previous work,[13,14] we reported the structure and properties of nine compositions in the $(1-x-y)(Bi_{1/2}Na_{1/2})TiO_3-xBaTiO_3-y(K_{0.5}Na_{0.5})NbO_3$ lead-free system with $x=0.05$, 0.06, 0.07 and $y=0.01$, 0.02, 0.03. Conventional laboratory x-ray diffraction revealed a pseudocubic crystal structure for all compositions, and TEM examination indicated the absence of prominent ferroelectric domains in some compositions. In the present study, large ferroelectric domains were observed in most grains in BNT-FE, as shown in Fig. 2(a). Some domains are exemplarily marked with bright arrows. In contrast to this, the absence of large ferroelectric domains is confirmed in the BNT-AFE sample. In addition, many defects with dimensions around 20 nm were found in most large grains in this ceramic. Two of these defects are indicated by bright arrows in Fig. 2(b). The nature of these defects is still unclear and detailed examination and analysis are currently underway.

The selected area electron diffraction patterns allow for the distinction between the two ceramics. As shown in Fig. 2(c), BNT-FE displays sharp and strong $(\frac{1}{2}\frac{1}{2}\frac{1}{2})_c$-type superlattice diffraction spots in the $\langle 110\rangle_c$-zone axis pattern. In contrast, these superlattice spots are very weak in the BNT-AFE ceramic, but there are additional $(\frac{1}{2}\frac{1}{2}0)_c$-type superlattice diffraction spots in the $\langle 100\rangle_c$-zone axis pattern. The presence of superlattice spots in perovskite oxides indicate a doubling of the unit cell and it has been attributed to either cation ordering or oxygen octahedra tilting.[26,27] Since cation ordering is not likely to occur in these ceramics,[28–30] the electron diffraction results indicate that BNT-FE is rhombohedrally distorted, most likely with the $R3c$ space group,[28–30] and BNT-AFE displays a pseudocubic perovskite structure with, at the moment, unknown octrahedra tilting. A mixed tilting system, either a combination of in-phase and antiphase tilting or a two phase mixture of one antiphase and one in-phase tilting, is possible.

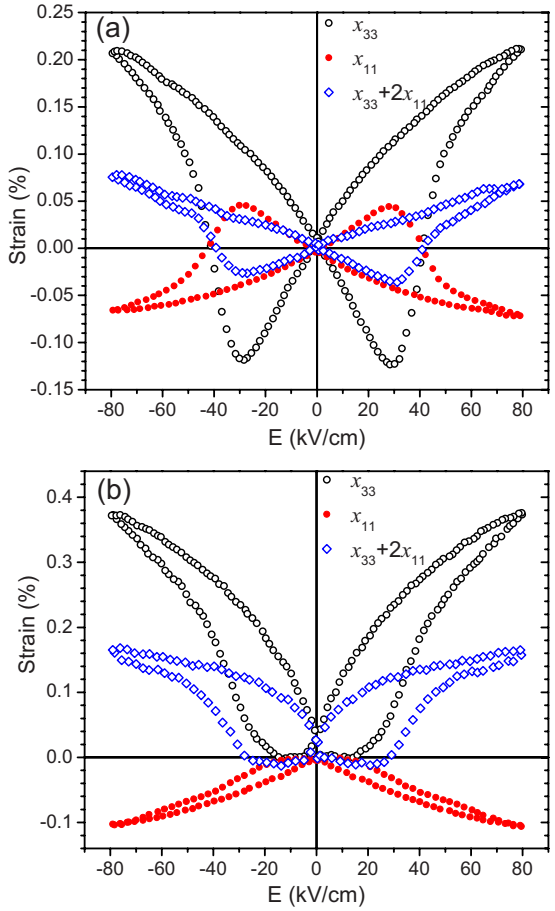

FIG. 3. (Color online) The electric field-induced longitudinal strain x_{33}, transverse strain x_{11}, and volume strain $(x_{33}+2x_{11})$ at room temperature measured at 50 mHz in (a) the BNT-FE ceramic and (b) the BNT-AFE ceramic.

B. Piezoelectricity

Figure 3 displays the electric field-induced longitudinal strain x_{33}, transverse strain x_{11}, and volume strain $(x_{33}+2x_{11})$ for both compositions. Under electrical loads, BNT-FE, which exhibits large ferroelectric domains, does not elongate as much as BNT-AFE. At the maximum field of 80 kV/cm, $x_{33}=+0.22\%$ and $x_{11}=-0.07\%$ in BNT-FE [Fig. 3(a)]. Much larger strains [Fig. 3(b)] were observed in BNT-AFE ($x_{33}=+0.38\%$ and $x_{11}=-0.10\%$). In addition, both x_{33} and x_{11} display a much more severe hysteretic behavior in BNT-FE than in BNT-AFE. Another difference between the two compositions is that in BNT-AFE, x_{33} displays almost exclusively positive values (elongation) and x_{11} displays only negative values (contraction), while in BNT-FE, both positive and negative values are seen in x_{33} and x_{11}. From the volume strain $(x_{33}+2x_{11})$ data, it is evident that volume expansion under electric fields is primarily observed in BNT-AFE, while both volume expansion and volume contraction (a volume strain of -0.04% at coercive field) are displayed

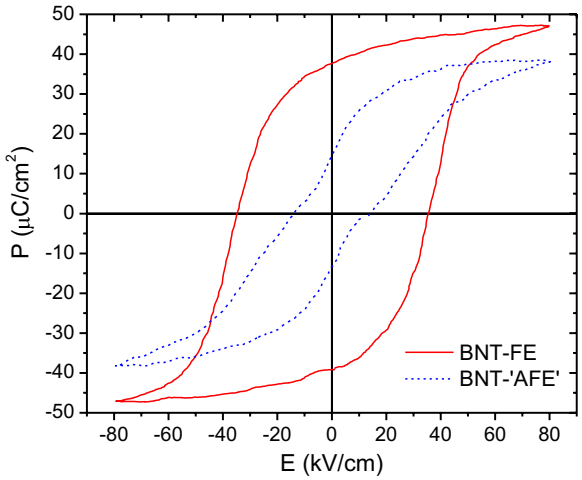

FIG. 4. (Color online) The polarization vs electric field hysteresis loop measured at room temperature at 50 mHz in the BNT-FE ceramic and the BNT-AFE ceramic.

by BNT-FE. Furthermore, portions of the $(x_{33}+2x_{11})$ versus E curve in Fig. 3(a) for BNT-FE display a rather linear relation. The gradual change in the strains with applied electric fields in BNT-AFE, the supposedly antiferroelectric lead-free ceramic, is in sharp contrast to the abrupt jump in electric field-induced strains in $PbZrO_3$-based antiferroelectric oxides.[31]

C. Ferroelectricity

Accompanying the strain developed under electric field E is the electrical polarization P. The hysteretic relation between P and E is displayed in Fig. 4. A well-defined loop is found for BNT-FE, and a pinched one is recorded for BNT-AFE. Much greater values of E_c (35.2 kV/cm) and P_r (38.5 $\mu C/cm^2$) are measured for BNT-FE than for BNT-AFE (13.6 kV/cm and 14.2 $\mu C/cm^2$, respectively).

The solid solution system under examination exhibits a transition from the ferroelectric to a nonferroelectric phase. The transition temperature, referred to as depolarization temperature T_d, can be shifted with $(K_{0.5}Na_{0.5})NbO_3$ addition. This is depicted in Fig. 5, which shows the change in the

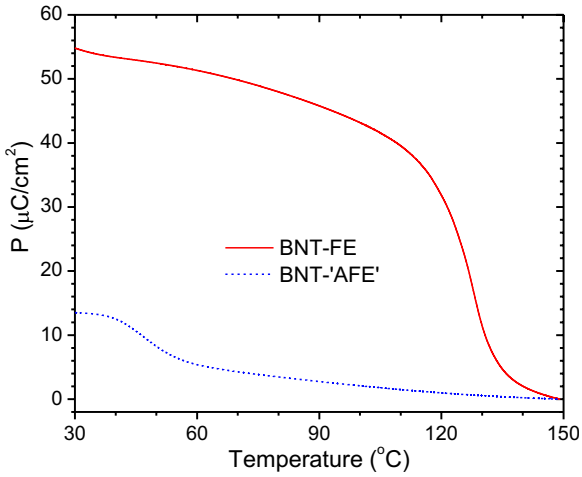

FIG. 5. (Color online) The thermal depolarization process in poled BNT-FE and BNT-AFE ceramics.

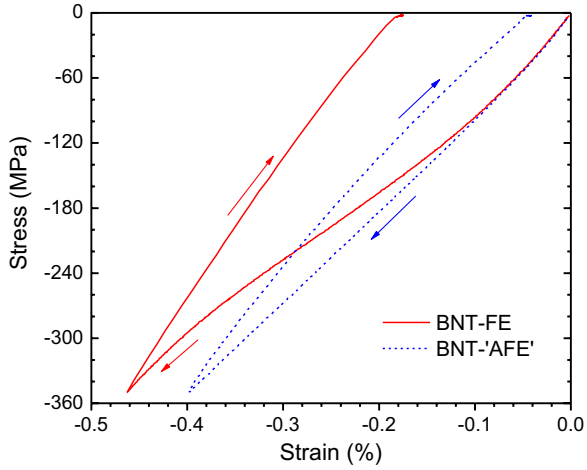

FIG. 6. (Color online) The ferroelastic deformation of the BNT-FE and the BNT-AFE ceramics at room temperature.

remanent polarization of a poled sample of each composition with temperature upon heating. T_d is determined as the temperature where the thermal depolarization current peaks. T_d = 128 °C was measured for BNT-FE. For BNT-AFE, there is much less polarization even at room temperature, but a noticeably further decrease is observed at 46 °C. As shown in Fig. 5, P decreases dramatically at temperatures near T_d. However, electrical polarization persists to temperatures well above T_d, especially in the BNT-AFE ceramic. This seems to be associated with the fact that the ferroelectric phase coexists with the nonferroelectric phase, considered to be antiferroelectric, in a temperature window from 255 to 400 °C in the base compound $(Bi_{1/2}Na_{1/2})TiO_3$.[30] From Fig. 5, the remanent polarization is 54.8 $\mu C/cm^2$ in BNT-FE and 13.6 $\mu C/cm^2$ in BNT-AFE at 30 °C. These values are comparable to the remanent polarization values P_r measured from the hysteresis loops shown in Fig. 4.

D. Ferroelasticity

The stress-strain curves for the mechanical deformation under uniaxial compression of as-sintered ceramics are displayed in Fig. 6. During loading, the BNT-FE ceramic exhibits predominantly linear behavior up to 100 MPa, while at higher stresses a significant nonlinear behavior was observed. A strain of 0.46% is reached at the maximum stress of 350 MPa. The loading curve for BNT-AFE is quite straight, and the strain developed under the maximum mechanical load is 0.40%. Furthermore, both ceramics exhibit only very limited backswitching on unloading. A much greater residual strain (0.18%) remains in BNT-FE as compared to BNT-AFE (0.05%) right after the mechanical load is removed. Young's modulus for both materials was initially (105 ± 5) GPa and was reduced to (90 ± 5) GPa at the maximum load after ferroelastic switching.

E. Combined electromechanical loading

Uniaxial compressive stress restricts field-induced ferroelectric domain switching for the case of the ferroelectric material. For the case of the nonferroelectric material, the field-induced phase transition should be adversely affected

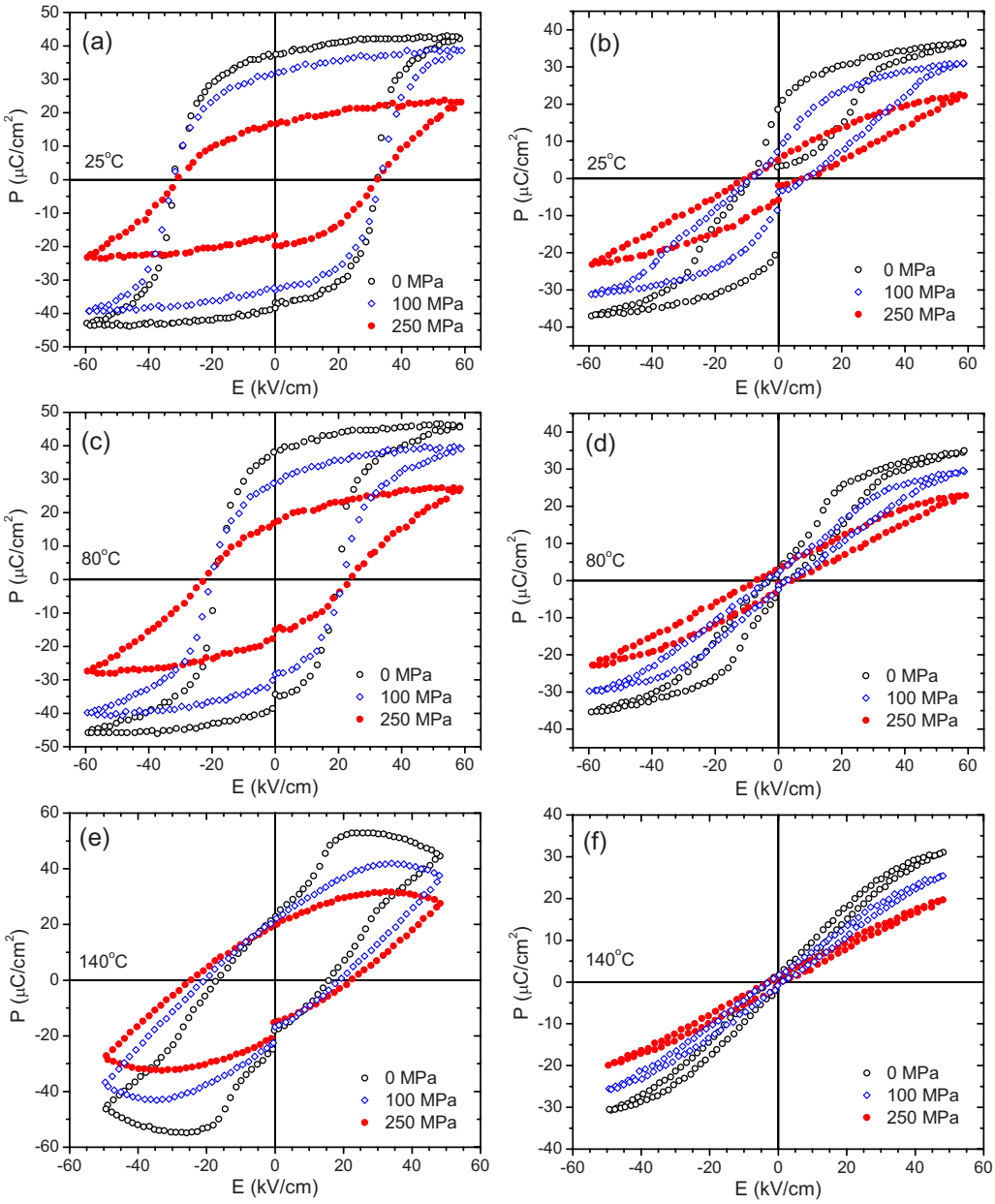

FIG. 7. (Color online) The effect of uniaxial compressive pre-stresses on the polarization hysteresis loops in BNT-FE at (a) 25 °C, (c) 80 °C, and (e) 140 °C and in BNT-AFE at (b) 25 °C, (d) 80 °C, and (f) 140 °C.

by the hydrostatic component (σ_h) of the uniaxially applied stress (σ_a). The effects of uniaxial compressive prestresses on the polarization were evaluated at 25, 80, and 140 °C for both BNT-FE and BNT-AFE. The temperature 25 °C is below the T_d for BNT-FE, while for BNT-AFE at this temperature, a mixture of ferroelectric and nonferroelectric phases is present. The polarization hysteresis loops under the peak field of 60 kV/cm at this temperature are displayed in Figs. 7(a) and 7(b). For BNT-FE, the maximum polarization $P_{\max}$ as well as the remanent polarization P_r were evidently suppressed by uniaxial compressive stress, while the coercive field E_c almost remains the same. However, a well defined hysteresis loop with a P_r of 17.6 $\mu C/cm^2$ persists even at 250 MPa. For BNT-AFE, $P_{\max}$ and P_r were also suppressed by the applied compressive stress.

The temperature 80 °C is still below the T_d of BNT-FE, but above the T_d of BNT-AFE. The uniaxial compressive prestress shows similar effects on polarization to that at 25 °C in BNT-FE, as shown in Fig. 7(c). The coercive field E_c is smaller than that at 25 °C and increases with increasing compressive stresses. Again, a large P_r (16.9 $\mu C/cm^2$) is still observed even at 250 MPa. The BNT-AFE ceramic is completely in the nonferroelectric phase at 80 °C. However, well-defined double hysteresis loops that are characteristic of $PbZrO_3$-based antiferroelectric ceramics were not observed in BNT-AFE. Instead, pinched hysteresis loops with minimum P_r were recorded [Fig. 7(d)]. With increasing compressive stresses, $P_{\max}$ was reduced while P_r is more or less unchanged. Compared to the hysteresis loops at 25 °C displayed in Fig. 7(b), a significant reduction in P_r is observed, which is consistent with the thermal depolarization result shown in Fig. 5.

The temperature 140 °C is above the T_d of both ceramics. Therefore, both BNT-FE and BNT-AFE are presumably

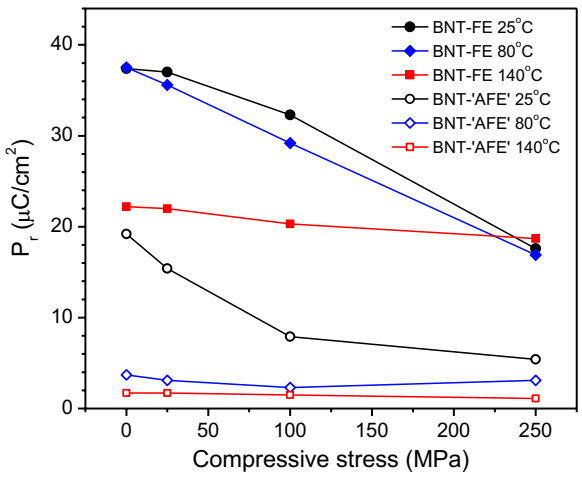

FIG. 8. (Color online) The change in remanent polarization P_r as a function of compressive prestress at different temperatures in BNT-FE and BNT-AFE.

in the nonferroelectric phase. A severely distorted hysteresis loop was observed at 0 MPa at this temperature for BNT-FE, as shown in Fig. 7(e). The maximum polarization P_{max} does not occur at the maximum electric field, which indicates that BNT-FE becomes lossy at this temperature. When the uniaxial compressive prestress increases, significant suppression of P_{max} is evident. However, the suppression of P_r is not nearly as significant. At the same time, an increase in the coercive field E_c is observed. In contrast, the BNT-AFE ceramic at 140 °C shows hysteresis loops that are characteristic of relaxor ferroelectrics, and the applied compressive stress reduces the slope, as shown in Fig. 7(f).

The change in the remanent polarization P_r as a function of applied compressive stresses at different temperatures for both ceramics is summarized in Fig. 8. Significant reduction in P_r with increasing mechanical stresses is observed in BNT-FE at 25 and 80 °C and in BNT-AFE at 25 °C. It is quite stable against compressive stresses in BNT-FE at 140 °C and in BNT-AFE at 80 and 140 °C.

IV. DISCUSSION

Our previous studies indicate that BNT-FE is ferroelectric while BNT-AFE is largely nonferroelectric at room temperature.[13,14] In the present study, the BNT-FE ceramic shows all the characteristics of a normal ferroelectric: micrometer-sized ferroelectric domains, apparent rhombohedral distortion, significant ferroelastic deformation, square *P-E* hysteresis loops, and an abrupt thermal depolarization process. Ferroelastic domain switching in BNT-FE exhibits quite different behaviors as compared to both soft and hard lead zirconate titanate (PZT).[17,18] In PZT, domain switching occurs in a comparatively narrow range of applied stress, while in BNT-FE, switching occurs over a very wide stress range, being most active at around 200 MPa. The resistance for ferroelastic domain switching in BNT-FE is much higher than in hard PZT ceramics (~100 MPa).[17,18] Consistent with this, the domain switching resistance under electric fields (indicated by the coercive field E_c) in BNT-FE is also more than twice as large as in hard PZT ceramics (35 kV/cm versus16 kV/cm).[17] The combination of the large electric field-induced strain and the high resistance of ferroelastic domain switching makes the BNT-FE ceramic promising for actuator applications, where a large blocking stress is desired. The ferroelastic data shown in Fig. 6 indicate that there is still a considerable amount of domain switching even at a compressive stress of 250 MPa. Correspondingly, a well-defined *P-E* hysteresis loop with a large P_r (17.6 $\mu C/cm^2$) persists at 250 MPa prestress at room temperature [Fig. 7(a)]. BNT-FE at both room temperature and 80 °C has a comparable remanent polarization to soft PZT,[19] and it displays a similar linear decrease with respect to the applied uniaxial stress. However, while soft PZT loses half of its remanent polarization already at 50 MPa of uniaxial stress,[19] BNT-FE is capable of sustaining up to 250 MPa prestress at half of its original remanent polarization.

The nonferroelectric BNT-AFE ceramic is quite distinct from $PbZrO_3$-based antiferroelectric ceramics. It neither displays the hierarchical antiferroelectric domain structure nor shows the well-defined double hysteresis loops.[32] The thermal depolarization data shown in Fig. 5 suggest that it is actually a mixture of ferroelectric and nonferroelectric phases. Such a two-phase coexistence has been acknowledged before in the base compound $(Bi_{1/2}Na_{1/2})TiO_3$.[30] If we assume that the ferroelectric phase in BNT-AFE possesses the same polarization as in BNT-FE, we can estimate the volume fractions of the ferroelectric and nonferroelectric phases at about 25% and 75%, respectively, in the BNT-AFE ceramic at room temperature. The electric field-induced antiferroelectric-to-ferroelectric phase transition was suggested to be responsible for the pinched *P-E* hysteresis loops and the large positive longitudinal strain x_{33}. It is interesting to note from Fig. 3 that the maximum x_{33} in BNT-AFE is about 75% higher than that in BNT-FE. The transition from a pinched shape of the hysteresis to a regular slim hysteresis loop at elevated mechanical load at both 25 and 80 °C [Figs. 7(b) and 7(d)] indicates that the uniaxial compressive prestress of 250 MPa subdues the transition from the nonferroelectric to the ferroelectric phase but does not prevent domain switching in the volume containing the ferroelectric phase. We speculate that the higher x_{33} in BNT-AFE is responsible for this. At 140 °C, BNT-FE is also expected to be a mixture of ferroelectric and nonferroelectric phases. Similarly, the uniaxial compressive prestress removes the distortion from the hysteresis loop [Fig. 7(e)]. As demonstrated by the ferroelastic test data shown in Fig. 6, the nonferroelectric phase displays only very weak ferroelasticity. This is an indication that the nonferroelectric phase is, in fact, not a regular antiferroelectric. This observation is consistent with the results summarized in Fig. 8: At temperatures above T_d, the remanent polarization P_r is insensitive to the compressive prestress.

In fact, the only evidence supporting the antiferroelectric nature of the nonferroelectric phase are the pinched polarization and strain hysteresis loops.[13,14] The pseudocubic structure and the absence of large antiferroelectric domains suggest that the BNT-AFE ceramic rather bear characteristics of relaxor ferroelectrics. Indeed, the *P-E* hysteresis loops in BNT-AFE at 140 °C are very much like the ones observed in

$Pb(Mg_{1/3}Nb_{2/3})O_3$-based relaxor ferroelectric ceramics.[33] In addition, the fact that the electric field-induced transverse strain x_{11} in BNT-AFE remains negative irrespective of the field polarity [Fig. 3(b)] is suggestive of a relaxor ferroelectric displaying an electrostrictive behavior.[34] In ceramics with an electric field-induced antiferroelectric-to-ferroelectric transition, an expansion in the transverse direction (positive x_{11}) is usually observed.[31]

It should be pointed out that the complexity and confusion in BNT-AFE trace their origin back to the base compound $(Bi_{1/2}Na_{1/2})TiO_3$. Earlier x-ray[28] and neutron[29] structural studies indicate that there are no antiparallel cation displacements in $(Bi_{1/2}Na_{1/2})TiO_3$, and the term "diffused antiferroelectric" was used to describe the mixed relaxor and antiferroelectric behavior.[29] Later, contradictory observations were reported in a detailed neutron diffraction study where antiparallel cation displacements were found in the antiferroelectric tetragonal phase.[30] In addition, the tetragonal phase was reported to coexist with the ferroelectric rhombohedral phase over a wide temperature range. However, a recent electron diffraction study on $(Bi_{1/2}Na_{1/2})TiO_3$ revealed that the rhombohedral phase with large ferroelectric domains was progressively disrupted by an intermediate modulated phase with an orthorhombic symmetry when heated.[23] Similar modulations were not observed in our BNT-AFE ceramic.

V. CONCLUSIONS

Our experimental investigations revealed a strong ferroelastic behavior in the lead-free piezoelectric BNT-FE ceramic. The switching of ferroelastic domains is most active around a uniaxial compressive stress of 200 MPa and persists up to stresses beyond 300 MPa. Under electric fields, significant ferroelectric domain switching is still observed even when the ceramic is subjected to a 250 MPa uniaxial compressive prestress. The results suggest that the lead-free piezoelectric BNT-FE ceramic outperforms PZT ceramics in actuator applications where a high blocking stress is required. In contrast, the BNT-AFE ceramic shows a very limited ferroelastic deformation under mechanical stress. This is probably due to the low volume fraction of the ferroelectric ferroelastic phase. The nonferroelectric phase does not seem to contribute to the ferroelastic behavior, presenting an argument against the antiferroelectric nature of this phase. However, the volume fraction of the ferroelectric phase can be increased by electric fields through a field-induced phase transition at room temperature, which is accompanied by the development of a large longitudinal strain. It appears that this electric field-induced phase transition can be suppressed by uniaxial compressive prestresses above 100 MPa. The BNT-AFE ceramic was described as antiferroelectric previously due to the presence of pinched polarization hysteresis loops. However, a number of other features such as its pseudocubic structure, almost linear elastic behavior, and complete transverse contraction rather seem to suggest a relaxor ferroelectric behavior.

ACKNOWLEDGMENTS

This work was supported by the Deutsche Forschungsgemeinschaft (DFG) under Grant Nos. SFB 595 and GR2722/4-1.

[1] B. Jaffe, W. R. Cook, and H. Jaffe, *Piezoelectric Ceramics* (Academic, New York, 1971).
[2] J. Rödel, W. Jo, K. Seifert, E. M. Anton, T. Granzow, and D. Damjanovic, J. Am. Ceram. Soc. **92**, 1153 (2009).
[3] T. Takenaka and K. Sakata, Ferroelectrics **95**, 153 (1989).
[4] T. Takenaka, K. Maruyama, and K. Sakata, Jpn. J. Appl. Phys., Part 1 **30**, 2236 (1991).
[5] Y. M. Chiang, G. W. Farrey, and A. N. Soukhojak, Appl. Phys. Lett. **73**, 3683 (1998).
[6] X. X. Wang, H. L. W. Chan, and C. L. Choy, Solid State Commun. **125**, 395 (2003).
[7] H. Nagata, M. Yoshida, Y. Makiuchi, and T. Takenaka, Jpn. J. Appl. Phys., Part 1 **42**, 7401 (2003).
[8] Y. Saito, H. Takao, T. Tani, T. Nonoyama, K. Takatori, T. Homma, T. Nagaya, and M. Nakamura, Nature (London) **432**, 84 (2004).
[9] M. Matsubara, T. Yamaguchi, W. Sakamoto, K. Kikuta, T. Yogo, and S. Hirano, J. Am. Ceram. Soc. **88**, 1190 (2005).
[10] R. Z. Zuo, X. S. Fang, and C. Ye, Appl. Phys. Lett. **90**, 092904 (2007).
[11] S. Teranishi, M. Suzuki, Y. Noguchi, M. Miyayama, C. Moriyoshi, Y. Kuroiwa, K. Tawa, and S. Mori, Appl. Phys. Lett. **92**, 182905 (2008).
[12] S. T. Zhang, A. B. Kounga, E. Aulbach, H. Ehrenberg, and J. Rödel, Appl. Phys. Lett. **91**, 112906 (2007).
[13] S. T. Zhang, A. B. Kounga, E. Aulbach, T. Granzow, W. Jo, H. J. Kleebe, and J. Rödel, J. Appl. Phys. **103**, 034107 (2008).
[14] S. T. Zhang, A. B. Kounga, E. Aulbach, W. Jo, T. Granzow, H. Ehrenberg, and J. Rödel, J. Appl. Phys. **103**, 034108 (2008).
[15] J. E. Daniels, W. Jo, J. Rödel, and J. L. Jones, Appl. Phys. Lett. **95**, 032904 (2009).
[16] W. Jo, T. Granzow, E. Aulbach, J. Rödel, and D. Damjanovic, J. Appl. Phys. **105**, 094102 (2009).
[17] H. Cao and A. G. Evans, J. Am. Ceram. Soc. **76**, 890 (1993).
[18] Q. M. Zhang, J. Zhao, K. Uchino, and J. Zheng, J. Mater. Res. **12**, 226 (1997).
[19] D. Zhou, M. Kamlah, and D. Munz, J. Eur. Ceram. Soc. **25**, 425 (2005).
[20] D. Viehland, J. Am. Ceram. Soc. **89**, 775 (2006).
[21] G. Yang, Z. Yue, Y. Ji, and L. Li, J. Appl. Phys. **104**, 074116 (2008).
[22] M. Unruan, R. Wongmaneerung, A. Ngamjarurojana, Y. Laosiritaworn, S. Ananta, and R. Yimnirun, J. Appl. Phys. **104**, 064107 (2008).
[23] V. Dorcet, G. Trolliard, and P. Boullay, Chem. Mater. **20**, 5061 (2008).
[24] D. C. Lupascu, E. Aulbach, and J. Rödel, J. Appl. Phys. **93**, 5551 (2003).
[25] K. G. Webber, R. Zuo, and C. S. Lynch, Acta Mater. **56**, 1219 (2008).
[26] X. Zhao, W. Qu, and X. Tan, J. Am. Ceram. Soc. **91**, 3031 (2008).
[27] W. Qu, X. Tan, and P. Yang, Microsc. Res. Tech. **72**, 216 (2009).
[28] J. A. Zvirgzds, P. P. Kapostins, and J. V. Zvirgzde, Ferroelectrics **40**, 75 (1982).
[29] S. B. Vakhrushev, V. A. Isupov, B. E. Kvyatkovsky, N. M. Okuneva, I. P. Pronin, G. A. Smolensky, and P. P. Syrnikov, Ferroelectrics **63**, 153 (1985).
[30] G. O. Jones and P. A. Thomas, Acta Crystallogr., Sect. B: Struct. Sci. **58**, 168 (2002).
[31] X. Tan, W. Jo, T. Granzow, J. Frederick, E. Aulbach, and J. Rödel, Appl. Phys. Lett. **94**, 042909 (2009).
[32] H. He and X. Tan, Phys. Rev. B **72**, 024102 (2005).
[33] W. Qu, X. Zhao, and X. Tan, Appl. Phys. Lett. **89**, 022904 (2006).
[34] K. Uchino, S. Nomura, L. E. Cross, R. E. Newnham, and S. J. Jang, J. Mater. Sci. **16**, 569 (1981).